Controller Design for Ventricular Assist Devices

Guruprasad A. Giridharan* and Mikhail Skliar†
Department of Chemical and Fuels Engineering
University of Utah
Salt Lake City, UT 84112

Abstract

In this paper, an integrated model of the human circulatory system with a brushless DC axial flow ventricular assist device (VAD) was developed. The resulting nonlinear hybrid model is then used to design the VAD feedback control system. The VAD controller is designed to maintain a physiologically motivated perfusion; it is tested using computer simulations of different scenarios ranging from the normal heart to the left heart asystole.

Keywords

Circulatory system model, Ventricular assist devices, Physiological control of rotary blood pumps

Introduction

Ventricular assist devices (VAD) have been in use for many years as a bridge to transplantation (Olsen, 1999) and hold a potential to become a long-term alternative to donor heart transplantation. VADs are mechanical support systems used in parallel with the failed heart to reduce the heart's workload.

Currently, a control system for continuous-flow VADs, which automatically responds to physiological cardiac demand, does not exist. In hospitals, the flow rate generated by the continuous flow VAD, such as the DeBakey pump, is selected manually by a physician or trained support personnel. Mobile patients can operate implanted continuous flow VADs in one of two ways: "automatic" or manual. During automatic control, the patient, following guidelines provided by the doctor, sets the desired pump rpm depending on the level of physical activity. The VAD controller automatically adjusts the current and voltage applied to the pump to achieve the desired rpm setpoint. A feedback system based on physiological measurements (such as pressures, flows, O_2 saturation, etc.) is currently not available. In manual mode, the patient directly adjusts the pump rpm by "twisting the knob" until the comfort level of perfusion is achieved.

A recent paper (Waters et al., 1999) is representative of the current state-of-the-art in developing an improved control of continuous flow VADs; in this paper, a PI controller was designed using a simple computer model of the circulatory system. The assumptions made by Waters et al. (1999) are unrealistic, including continuous flow throughout the circulatory system, no heart valves and linear correlation between pump generated pressure difference, ΔP, and pump voltage, current and rpm. Further research is clearly needed before a physiologically motivated continuous VAD control system can be developed for devices used in patients.

The selection of an adequate model, which avoids the overwhelming complexity of the full-scale CFD model, but retains all relevant characteristics of the circulatory system motivated our selection of the network-type circulation model. However, unlike the previous work by Waters et al. (1999), where the linear model with continuous flow throughout the system was assumed, we preserve such characteristics as nonlinearity, pulsativity and discontinuity due to the effects of the heart valves.

The selected control objective is to maintain the pressure difference between the left heart (LH) and the aorta close to the specified reference pressure. We show that this control objective leads to an adequate and physiologically motivated perfusion. At the same time, the simplicity of the objective allows for an implementation of simple control laws. In particular, a PI controller, developed to vary the VAD electrical current to minimize the difference between the reference and the actual differential pressure, results in a surprisingly good perfusion in vastly different clinical cases, ranging from the normal heart to a completely failed (asystolic) left heart.

During the development of the feedback system, we assumed that two implanted pressure sensors and an rpm sensor were available for the feedback. However, the need for implantable pressure sensors (the least reliable components) can potentially be eliminated by using readily available measurements of the pump rpm, voltage, and current to estimate the differential pressure between the left heart and the aorta.

Model Development

The model used in the controller design incorporates a model of the human circulatory system with a model of the continuous flow left ventricular assist device (LVAD).

Model of the Circulatory System

The Utah Circulation Model (UCM) is a network type model, which subdivides the human circulatory system into an arbitrary number of lumped parameter blocks, each characterized by its own resistance, compliance, pressure and volume of blood. In its simplest configuration, the UCM has eleven elements: 4 heart valves, and 7 blocks including the left heart, the right heart (RH), pulmonary and systemic circulation, the vena cava and

*gurug@eng.utah.edu
†mikhail.skliar@m.cc.utah.edu

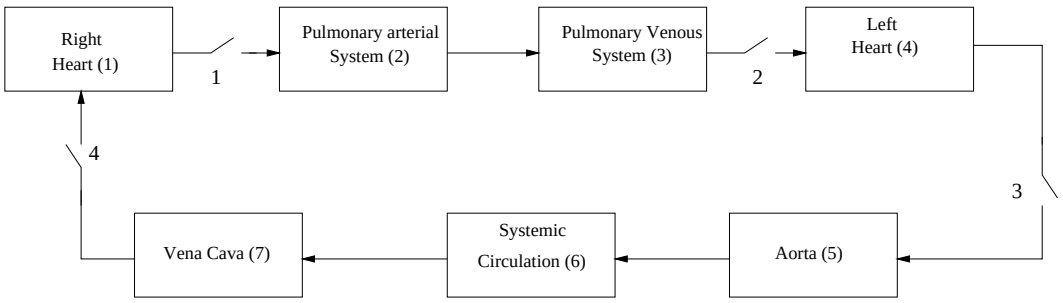

Figure 1: Schematic of the UCM.

the aorta, Figure 1. An arbitrary modeling detail can be achieved by increasing the number of blocks. The model was developed under the typical (McLeod, 1972) assumptions that blood is a Newtonian fluid, heart valves open and close instantaneously, and constant flow resistance in all blocks. Except for the heart blocks, the compliance of all other blocks remains constant.

Each block of the model is characterized by its resistance, R, to the flow, F, and its compliance, C, which characterizes the ability of a block to store a volume of blood, V. Two idealized elements, resistance and storage, are used to characterize each block. The storage element provides zero resistance to the flow, while the resistive element has zero volume. The resistance of the n-th block, R_n, is defined as a proportionality constant between pressure drop and blood flow across the block so that flow rates into and out of the block are given by

$$F_n^{in} = \frac{P_{n-1} - P_n}{R_{n-1}}, \quad F_n^{out} = \frac{P_n - P_{n+1}}{R_n}, \qquad (1)$$

where P_n is the pressure at the inlet of the n-th block, etc. The compliance, C_n, is defined as the ratio between the inlet pressure, P_n, to the stored volume of blood, V_n: $C_n = \frac{V_n}{P_n}$.

We further classify blocks as passive and active. Active blocks represent heart chambers; they are characterized by the varying compliance within each cardiac cycle. The rest of the blocks are referred to as passive. The varying compliance of the active blocks is responsible for the progression of a heartbeat. Figure 2 gives the typical value of the compliance of an active block used in the simulations.

The volume of blood in each block is described by a differential equation, which is an expression for the macroscopic material balance for a block.

The resistances and compliances will differ in different patients. In this work, typical values of Cs and Rs were assumed for all passive and active blocks. Parameters of the active blocks were adjusted to reflect different pathological conditions during the evaluation of the VAD control system performance under different scenarios.

The UCM includes four heart valves. Introducing valve conductance of the i-th valve, C_i^h, as an inverse of

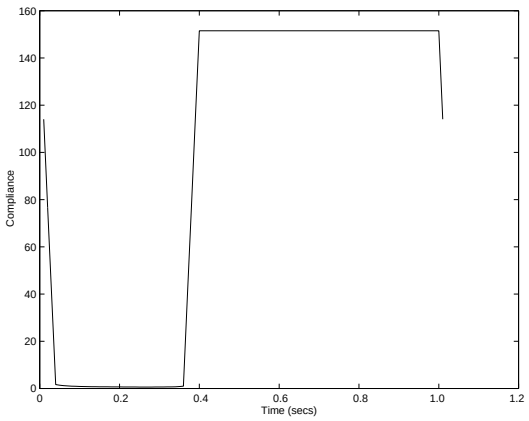

Figure 2: Typical compliance of an active block as a function of time.

the valve resistance, R_i^h, obtain: $C_i^h = \frac{1}{R_i^h} = c_i^h \delta_i$, $c_i^h = constant$, $i = \overline{1,4}$, where the Kronecker delta is a logical function of the differential pressure ΔP_i across the valve:

$$\delta_i = \begin{cases} 0 & \text{when } \Delta P_i \geq 0 \\ 1 & \text{when } \Delta P_i < 0 \end{cases}. \qquad (2)$$

The resulting model of the circulatory system now includes both dynamic and logical components, and is therefore, a hybrid system.

Model of the Axial Flow VAD

The integrated circulatory model includes a model of the axial flow LVAD, such as DeBakey LVAD, as an assist device. The LVAD is driven by a brushless DC motor. A typical brushless DC motor can be described by the following equations (Pillay and Krishnan, 1989):

$$J\frac{d\omega}{dt} = T_e - B\omega - T_p, \qquad (3)$$

where J is the inertia of the rotor, ω is the rotor speed in rads/sec, T_e is the motor torque, T_p is the load torque and B is the damping coefficient.

If the motor has a sinusoidal back EMF, the phase current also has a sinusoidal waveform. In this case

(Choi et al., 1997), the motor torque is related to the amplitude of the phase current, I, as

$$T_e = \frac{3}{2} K_B I, \tag{4}$$

where K_B is the constant of the back EMF. Following Choi et al. (1997), we adopt the following functional form for the correlation between the pump rotational speed, ω, generated flow rate, F_p, and the load torque:

$$T_p = a_0 \omega^3 + a_1 F_p \omega^2, \tag{5}$$

where a_0 and a_1 are correlation constants.

To obtain the LVAD model in the closed form, we need an additional correlation between the pump flow rate and the corresponding pressure rise across the pump, $\Delta P = P_5 - P_4$, and the rotational speed of the pump. Following Konishi et al. (1994), the following differential equation is used to describe the axial pump flow rate, and close the VAD model:

$$\frac{dF_p}{dt} = -\frac{b_0}{b_1} F_p - \frac{b_2}{b_1} \omega^2 + \frac{1}{b_1} \Delta P, \tag{6}$$

where b_0, b_1 and b_2 are experimental constants.

Model integration

In most cases, the assist device works in parallel with the natural heart taking blood from the LH and returning it to the aorta. Using the same block numbering as in Figure 1, we obtain the integrated model in the following form:

$$\begin{cases} \begin{bmatrix} \dot{\boldsymbol{v}} \\ \dot{F}_p \end{bmatrix} = \begin{bmatrix} \boldsymbol{A}_1 & \boldsymbol{A}_2 \\ & \boldsymbol{A}_3 \end{bmatrix} \begin{bmatrix} \boldsymbol{v} \\ F_p \end{bmatrix} + \begin{bmatrix} \mathbf{0} \\ -\frac{b_2}{b_1} \end{bmatrix} \omega^2 \\ \dot{\omega} = -\frac{B}{J}\omega - \frac{a_1}{J} F_p \omega^2 - \frac{a_0}{J}\omega^3 + \frac{3K_B}{2J} I, \end{cases} \tag{7}$$

where $\boldsymbol{v} = \{V_i | i = \overline{1,7}\}$, $\boldsymbol{A}_2 = [0\ 0\ 0\ -1\ 1\ 0\ 0]^T$, $\boldsymbol{A}_3 = [0\ 0\ 0\ -\frac{1}{b_1 C_4}\ \frac{1}{b_1 C_5}\ 0\ 0\ -\frac{b_0}{b_1}]$, and $\mathbf{0}$ is a zero vector of an appropriate dimension. In diagonal form $\boldsymbol{A}_1 = \text{diags}\{\frac{1}{C_1(R_7+R_4^h)}\ \mathbf{0\ 0\ 0\ 0}\ \boldsymbol{a}_1\ \boldsymbol{a}_2\ \boldsymbol{a}_3\ \mathbf{0\ 0\ 0\ 0}\ \frac{1}{C_7(R_7+R_4^h)}\}$,

$$\boldsymbol{a}_1 = \begin{bmatrix} \frac{1}{C_1(R_1+R_1^h)} \\ \frac{1}{C_2 R_2} \\ \frac{1}{C_3(R_3+R_2^h)} \\ \frac{1}{C_4(R_4+R_3^h)} \\ \frac{1}{C_5 R_5} \\ \frac{1}{C_6 R_6} \end{bmatrix}, \boldsymbol{a}_3 = \begin{bmatrix} \frac{1}{C_2(R_1+R_1^h)} \\ \frac{1}{C_3 R_2} \\ \frac{1}{C_4(R_3+R_2^h)} \\ \frac{1}{C_5(R_4+R_3^h)} \\ \frac{1}{C_6 R_5} \\ \frac{1}{C_7 R_6} \end{bmatrix}, \tag{8}$$

where $R_i^h = \frac{1}{c_i^h \delta_i}$, $i = \overline{1,4}$ describes the resistance of the i-th heart valve, and the main diagonal

$$\boldsymbol{a}_2 = \begin{bmatrix} -\frac{1}{C_1}\left(\frac{1}{R_7+R_4^h} + \frac{1}{R_1+R_1^h}\right) \\ -\frac{1}{C_2}\left(\frac{1}{R_1+R_1^h} + \frac{1}{R_2}\right) \\ -\frac{1}{C_3}\left(\frac{1}{R_2} + \frac{1}{R_3+R_2^h}\right) \\ -\frac{1}{C_4}\left(\frac{1}{R_3+R_2^h} + \frac{1}{R_4+R_3^h}\right) \\ -\frac{1}{C_5}\left(\frac{1}{R_4+R_3^h} + \frac{1}{R_5}\right) \\ -\frac{1}{C_6}\left(\frac{1}{R_5} + \frac{1}{R_6}\right) \\ -\frac{1}{C_7}\left(\frac{1}{R_6} + \frac{1}{R_7+R_4^h}\right) \end{bmatrix}. \tag{9}$$

Equation 7 is the nonlinear, time-varying, hybrid model of the circulatory system with LVAD; its dimension depends on the number of blocks used to model the human circulatory system, and is equal to 9 in the present case. The pump current, I, is the manipulated variable.

In this work, we assume that the rotational speed of the pump, ω, and the pressure difference between the left heart and the aorta are directly measured. The rpm sensor can be integrated into the VAD design, as is the case with the DeBakey pump. However, measurements of differential pressure require an implantation of two pressure sensors, thus motivating an effort in developing "sensorless" VAD control systems, which relies on the estimation of ΔP from readily available measurements of pump current I, voltage V and rotational speed ω.

The compliances and resistances may differ from patient to patient. The variations with time within a patient can also be substantial. A limited number of identification schemes were previously proposed (Yu et al., 1996), which unfortunately require the implantation of additional pressure and flow sensors.

VAD Control

Control Objective and Design

The significance of the VAD control cannot be overstated. Though the design of a VAD itself is critical to the long-term success of the mechanical implant, the control of a VAD determines the confidence of doctors and patients in mechanically supported perfusion as a permanent solution and an alternative to the donor heart transplantation. The key requirement for the control system is the adaptation of the VAD generated flow to the changing physiological requirements of the patient.

Maintaining a reference differential pressure is known to be an effective way to correctly adapt the cardiac output to the changing requirements of the body. Such adaptation is possible because the vascular bed resistance can increase or decrease by a factor of 2 to 5 (Waters et al., 1999); since the flow is directly proportional to ΔP and is inversely proportional to the vascular bed resistance, maintaining a constant ΔP with changing bed

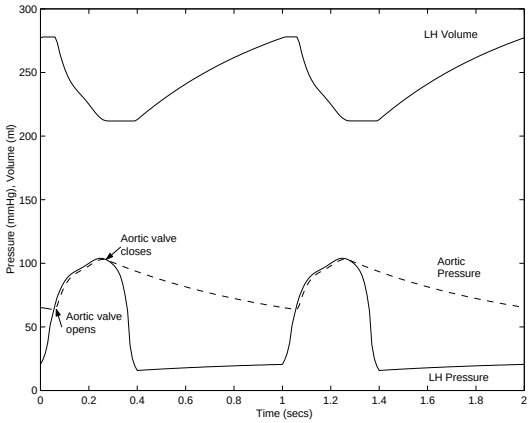

Figure 3: Volume and aortic pressure of a weakened heart.

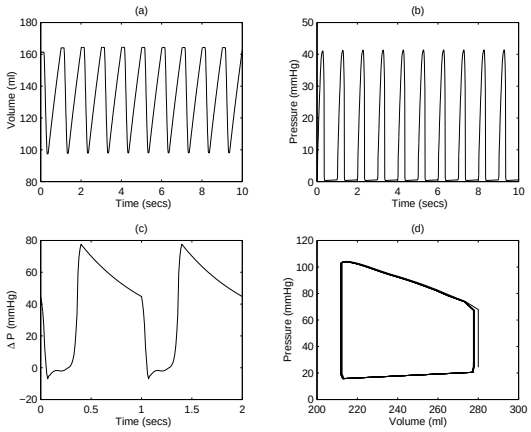

Figure 4: Characteristics of the weakened heart: (a) RH volume, (b) RH pressure, (c) ΔP between LH and aorta, (d) pressure-volume loop.

resistance can increase or decrease the flow rate by a factor of 2 to 5. A reference ΔP can be maintained by adjusting pump rpm within physiologically admissible limits despite changes in a patient's vascular resistance, stroke volume and pulse of the natural heart, all of which represent the response to natural regulatory mechanisms (Rao et al., 1999; Henson et al., 1995, 1994) to changing physiological cardiac output demands. By maintaining the prescribed ΔP we, in effect, synchronize the assist and natural perfusion, thus indirectly incorporating natural cardiovascular regulation into VAD control.

Controlling the ΔP also leads to relatively simple control algorithms and requires the implantation of only pressure sensors. An additional argument in favor of designing a ΔP controller is an observation that by controlling differential pressure we can ensure that pump rpm is maintained within limits dictated by physiological limitations related to possible collapse of the LH due to excessive suction, or back flow to the heart as a result of an inadequate pressure head developed by the VAD. The overall control problem can be formulated as the design of the feedback controller to regulate pump rpm within physiologically acceptable constraints, while minimizing the difference between the reference and the actual ΔP. Since pulsativity of the natural heart leads to the periodic changes in the ΔP, an additional objective is to keep oscillations of the pump rpm low, and, thus, increase pump life and the patient's comfort level. The formal expression of the control objective is to minimize the objective function J by selecting control input I subject to inequality constraints:

$$\min_I J = \int_0^t (\Delta P_r - \Delta P)^2 + r\dot{\omega}^2 dt, \qquad (10)$$

$$\omega_{min}(\boldsymbol{v}) \leq \omega(I) \leq \omega_{max}(\boldsymbol{v}), \qquad (11)$$

where $\boldsymbol{v}$ and ω must satisfy the system of nonlinear hybrid equations (7), and $r > 0$ is a user selectable weight.

The optimal solution to the formulated constrained quadratic optimal control problem for nonlinear hybrid systems is not known. Therefore, our approach is to select a fixed control structure followed by the optimization of the tuning parameters. In particular, for PI controller

$$I = K_P(\Delta P_r - \Delta P) + K_I \int_0^t (\Delta P_r - \Delta P)dt, \qquad (12)$$

the problem is to select the proportional and integral constants K_P and K_I, which minimize the objective function J. These constants were selected using an exhaustive, direct numerical search for the minimum of J for different weighting r until the desired tradeoff between speed of response and rpm oscillations was achieved. The maximum value of r was limited to insure that the upper constraint in (11) is not violated.

Simulation Results

The controller performance was evaluated under different clinical conditions, ranging from the healthy heart to an asystolic LH. Figures 3 and 4 show characteristics of the weakened heart without assistance, indicating lower than normal stroke volume of approximately 65 ml and the aortic systolic and diastolic pressures are around 105/65 mmHg. The LH volume is considerably higher than normal. The RH pressure is also much higher at the normal 40 mmHg (Figure 4b), and is typical for RH pressure with the failing left heart. Though not shown in the figures for the weakened heart, the simulation predicts edema in the pulmonary circulation. Figure 4d shows the work done by the weakened heart, which is less than the work typical of the healthy heart.

The effect of the LVAD with the designed PI controller was tested with the weakened heart, assuming the pulse rate was 60 beats per minute, and the same LVAD pa-

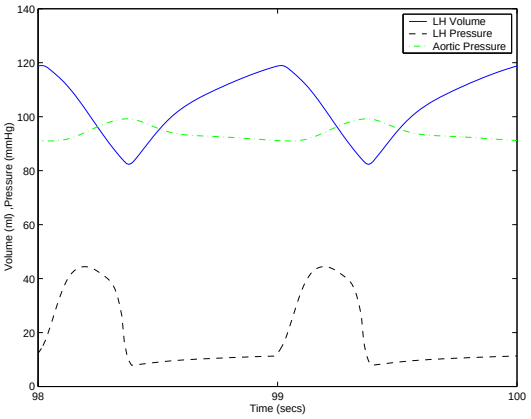

Figure 5: The LH characteristics and aortic pressure for a weakened heart with LVAD controlled by the PI controller.

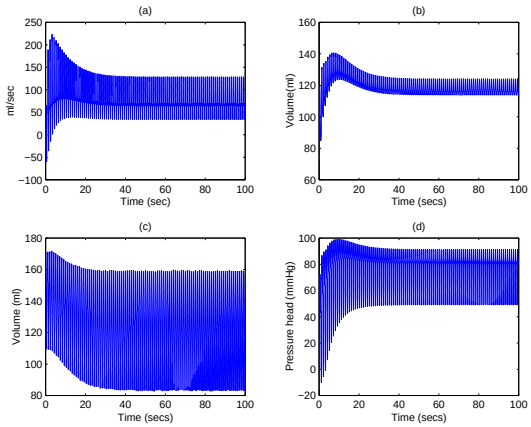

Figure 6: Weakened heart with LVAD assistance: (a) pump flow rate of the LVAD, (b) aorta volume, (c) RH volume and (d) ΔP between LH and aorta.

rameters as those used by Choi et al. (1997). At time $t = 0$, arbitrarily selected as the end of the diastole, the LVAD assistance was initiated with the reference differential pressure of 75 mmHg sent to the VAD controller. Initial VAD flow rate and rpm were set to zero, causing large initial back flow of blood to the left heart. Figures 5 and 6 show the results for the weakened heart assisted by the VAD with the designed controller. Figure 5 indicates a fairly constant aortic pressure 99/91 mmHg. The LH systolic and diastolic pressures are much closer to each other compared to a healthy heart with the LVAD. The volume of the LH with a VAD support reduces from 215/280 ml, observed without VAD assistance, to approximately 80/120 ml, which is in the normal range. The LH pressure is also reduced to about 45/12 mmHg. Though not shown in the figure, the RH pressure reduces to around 35/0 mmHg, which is within the normal range. The lung edema gradually reduces indicating an adequate perfusion. Figure 6 shows no pump back flow and the average pressure head of 75mmHg, which is the setpoint. After about 30 seconds the limit cycle is reached, at which time the rpm variations are reduced considerably, indicating inability of the weakened heart to produce high pressure variations.

Conclusions

The simulations show that maintaining an average pressure difference between the left heart and the aorta is an effective way to integrate the LVAD with the natural heart over a wide range of clinical conditions. The proposed control objective is effective in reflecting the physiological demands on perfusion, and simple enough to allow for simple control laws, which is a desirable feature because it simplifies FDA approval of a new device. However, the simplicity comes at a cost, since at least two implantable sensors are required. The feedback control without implantable sensors will necessitate the implementation of a more sophisticated control system, incorporating a ΔP estimator based on the measurements of the intrinsic pump characteristics. A further complication of adaptive control algorithms will be needed to account for inter- and intra- patient variability.

References

Choi, S., J. R. Boston, D. Thomas, and J. F. Antaki, Modeling and identification of an axial flow blood pump, In *Proceedings of the American Control Conference*, pages 3714–3715 (1997).

Henson, M. A., B. A. Ogunnaike, and J. S. Schwaber, "The Baroceptor Reflex: A Biological Control System with Applications in Chemical Process Control," *Ind. Eng. Chem. Res.*, **33**, 2453–2466 (1994).

Henson, M. A., B. A. Ogunnaike, and J. S. Schwaber, "Habituating Control Strategies for Process control," *AIChE J.*, **41**, 604–617 (1995).

Konishi, H., J. F. Antaki, J. R. Boston, J. P. Kerrigan, W. A. Mandarino, K. Yamaziki, M. Oe, P. Litwak, H. Borovetz, K. C. Butler, and R. L. Kormos, "Dynamic Systemic Vascular Resistance in Sheep Supported with Nimbus AxiPump," *ASAIO Journal*, **40**, M299–M302 (1994).

McLeod, J., "PHYSBE. A physiological simulation," *Simulation*, pages 152–156 (1972).

Olsen, D., "Sixth International Symposium for Rotary Blood Pumps," *Artificial Organs*, **26**, 475–476 (1999).

Pillay, P. and R. Krishnan, "Modeling, Simulation and Analysis of Permanent Magnet Motor Drives, Part 2: The Brushless DC Motor Drives," *IEEE Trans. Industrial Appl.*, **25** (1989).

Rao, R. R., B. Aufderheide, and B. W. Bequette, Multiple Model Predictive Control of hemodynamic variables, In *Proceedings of the American Control Conference*, pages 1253–1257 (1999).

Waters, T., P. Allaire, M. Adams, G. Bearnson, N. Wei, E. Hilton, M. Baloh, D. Olsen, and P. Khanwilkar, "Motor feedback physiological control for a continuous flow VAD," *Artificial Organs*, **23**, 480–486 (1999).

Yu, Y.-C., J. R. Boston, M. Simaan, and J. F. Antaki, Identification scheme for cardiovascular parameter estimation, In *13th IFAC World Congress*, pages 417–422 (1996).